12

Applying Atomic Force Microscopy to Studies in Cardiac Physiology

Jason J. Davis, Trevor Powell, and H. Allen O. Hill

1. Introduction

At the present time there exists a great deal of interest in the application of scanning probe microscopy methods to the imaging of cellular systems ***(1,2)***. It would now not be an exaggeration to state that atomic force microscopy (AFM), in particular, represents perhaps the most powerful means of structural/functional analysis at the level of a single live cell. In recent years this technology has been applied, amongst many other systems, to studies of bacterial flagella ***(3)***, erythrocytes ***(4)***, human platelets ***(5)***, endothelial cells ***(6)***, skin fibroblasts ***(7)***, plant cuticles ***(8)***, and cardiac myocytes ***(9)***. In resolution terms, perhaps the most impressive work is that of Engel et al. ***(10)***. Although not on whole cells (thereby greatly simplifying the experiment), molecular-level images of isolated cellular gap junctions, which play an important role in intracellular communication and signal transduction, have been obtained. More recently, experimental protocols have advanced to the point where it is possible to monitor, simultaneously, both cellular topography and ion channel flux ***(11)***. The ability to characterize functionally active cellular systems at a nanometre resolution under controlled fluid conditions has also been used in the monitoring of time-dependent cellular change ***(12,13)***.

Importantly, it is now generally accepted that, under appropriate imaging conditions, nanometre-resolved AFM experiments can be conducted with negligible levels of cellular damage ***(14)*** or, indeed, impaired cell physiological function ***(15)***. Despite this, however, under normal operational forces, one generally resolves submembrane structure rather than the structure of the membrane itself though the tip is only in direct contact with the latter. The plasma membrane offers little resistance to the loading force exerted by the scanning tip and is accordingly deformed as the tip traces out underlying internal struc-

From: *Methods in Molecular Biology, vol. 242: Atomic Force Microscopy: Biomedical Methods and Applications*
Edited by: P. C. Braga and D. Ricci © Humana Press Inc., Totowa, NJ

ture. Although this surface indentation has hindered high-resolution imaging of the extracellular surface, it can be used in the spatial characterization of internal cellular components. In summary, scanning probe methods, especially when combined with optical systems (confocal, total internal reflection, epifluorescence) provide a very powerful means of resolving the three-dimensional structure and dynamics of cellular systems under ambient and near-physiological conditions.

1.1. Cell Immobilization/Pretreatment

For any biological structure to be imaged satisfactorily by scanning probe methods, it must be immobile on an underlying substrate surface, under the typical lateral forces imparted by the scanning probe, at least for the duration of the scan. A range of methods has been developed for cellular immobilization. Most simply, the cells are dried down onto, or grown on, a suitable flat substrate surface; commonly mica (an aluminosilicate) or glass microscope slides. Nonspecific or electrostatic coatings, such as laminin or poly-L-lysine, are commonly applied to the bare surface to enhance the immobilization stability ***(16,17)***. Perhaps most simply, cells can be grown directly onto a substrate surface; these typically adhere robustly, although their structures are commonly perturbed (they may appear, for example, to be somewhat "spread" on the surface—a common observation with strong cell–substrate adhesion). Cells have also been entrapped in flexible, porous media ***(18,19)*** or imaged while embedded in a resin ***(20)***. It can be useful to adjust cellular mechanical properties (particularly in terms of membrane flexibility) by fixation (such as with glutaraldehyde). Such cell pretreatment generally enhances image resolution of the cytoskeleton. Related to this, the advantages associated with lowering imaging temperature, in terms of improved cellular robustness, have been noted ***(21)***.

1.2. Basic AFM Requirements

The substrate should have a surface roughness well below the vertical dimensions of the cell (and typically to be flat on a nanometre scale). In both contact and tapping force imaging it is commonly useful, if not critical, to quantify the forces imparted by the scanning tip (usually for the purposes of minimizing structural deformation of the sample). This is achieved, once the spring constant is determined (or estimated), through the generation of force–distance or amplitude–distance curves. The process of acquiring force–distance data over a cell surface can indeed be used to map cell mechanical properties with high spatial resolution ***(22,23)***. Note also that, under solution, it can be instructive to consider the effects of pH and ionic strength in minimizing electrostatic contributions to imaging force. Tip-sample adhesion forces are also highly dependent on the chemistry at the probe surface (be this silicon, silicon

nitride, or gold) and tip cleaning in oxidizing acids, or oxygen plasmas can be an effective way of attaining a reproducible behavior.

1.3. Cardiac Myocytes

The human heart is shaped like a blunt cone and is the size of a clenched fist, being some 12 cm long and 9 cm wide on average and weighs between 250 to 390 g in an adult male and about 200 to 250 g in a female. The mammalian heart is a hollow organ, containing four chambers, with a wall of muscle (or septum) dividing the organ vertically into a right and left heart. At the top of each half is an atrium (porch or antichamber) whereas below on each side is a ventricle (little belly). Within the walls of the heart are cells that both conduct electrical impulses and contract intermittently to raise blood pressure in the atria and ventricles. Particularly within the ventricular walls, these myocytes are arranged in bands as either spirals (like a turban) or in horizontal layers. The overall geometry of this contractile machinery subserves the function of impelling the blood from the left ventricle, or squeezing it out of the right half of the heart, into either the systemic or pulmonary circulations. The left ventricular wall is made up primarily of powerful circular musculature, sandwiched between layers of spiral muscles running from base to apex. The right ventricular wall consists almost exclusively of spiral muscles. This intricate myocardial anatomy, coupled with the distinct morphology and function of specialized component cells, often presents acute problems in the interpretation of experimental data obtained from the whole organ. Over the last 25 yr, individual myocytes isolated from the adult heart have become an important model system for a vast range of investigations concerning cardiac function in both the normal and diseased states. We shall demonstrate here that these myocytes are proving very useful in structure–function studies at resolutions obtainable with AFM.

2. Materials

1. High-purity buffer reagents; *N*-hydroxyethylpiperazine-*N*'-2-ethanesulfonate (HEPES), Dulbecco's minimal essential medium (DMEM).
2. Phosphate-buffered saline (PBS); (Sigma-Aldrich, cat. no P 0261).
3. High-purity water; 18.2 MΩ cm (Elga, UK).
4. 0.2 μm Syringe filters (Sterelin, UK).
5. Cleavable mica substrate (Agar Scientific, UK).
6. Glass microscope slides (Agar Scientific, UK).
7. Optical microscope (preferably of the Inverted configuration, with 60 to 100× objectives).
8. Scanning probe microscope capable of ambient and fluid contact and noncontact imaging.
9. Etched silicon and silicon nitride probes of appropriate spring constant and resonance frequency.

10. Perfusion apparatus; standard system for retrograde coronary perfusion (*see* **ref. *24*** for details).
11. DMEM solution (Life Technologies, UK).
12. Serum substitute; Ultroser G (Life Technologies, UK, cat. no. 81-003).
13. Collagenase; Worthington Type CLS I (Lorne Laboratories, UK).
14. Glutaraldehyde (Sigma-Aldrich).
15. 10-mL Sterile tubes (Sigma-Aldrich, cat. no. C-3084).

Centrifuge Note: with heart cells, small benchtop centrifuges are not to be recommended because their rapid acceleration can damage myocytes. Much better are the larger free-standing cooled types, such as the Mistral 4L.

3. Methods

The methods described below outline the process of (1) cell preparation, isolation, and electron microscopy characterization and (2) scanning force characterization.

3.1. Cell Preparation and Electron Microscopy Characterization

The detailed tissue dissociation protocols for the adult heart ***(24)*** will provide isolated myocytes suspended in Dulbecco's modified Eagle's medium supplemented with pyruvate and 10 m*M* HEPES to which has been added 2% (v/v) serum substitute. It is convenient to store cells at room temperature in sterile 10-mL tubes from Sigma-Aldrich. As long as standard precautions have been taken during isolation, these myocytes can be used for up to 24 h without any antibiotics. When incubation at 37°C is used (100% O_2 with HEPES media or 95 % O_2/5% CO_2 v/v if bicarbonate buffered only) then antibiotics must be added. Myocytes can be plated directly on to cover slips. Alternatively, cells can be fixed by first resuspending in Krebs' buffer (NaCl, 134.1; KCl, 5.4; $NaH_2PO_4.2H_2O$, 0.3; $MgCl_2$, 1; Na acetate.$3H_2O$, 5; Na pyruvate, 5; glucose, 11.1; HEPES, 5; all m*M*, pH adjusted to 7.4 with NaOH) and then adding 1 volume of myocytes to 2.5 % v/v glutaraldehyde in 1/3 Krebs' buffer. Though fixation is rapid, the cells are typically left for at least 30 min, then resuspended in phosphate-buffered saline and stored at 4°C. This fixative procedure has been designed to reduce the osmotic strength of the fixation solution and thereby reduce cell shrinkage.

High yields of ventricular myocytes from adult mammalian hearts are obtainable using retrograde (Langendorff) coronary perfusion of the whole organ, with fluids low in calcium, containing collagenase and protease. Details of the procedures have been presented elsewhere (*see*, for example, **ref. *24***; *see* **Note 1**). Examination of suspensions of isolated myocytes by bright-field light microscopy showed two distinct cell types; a dominant rod-shaped form together with a population of rounded cells (**Fig. 1**). It is clear from a number

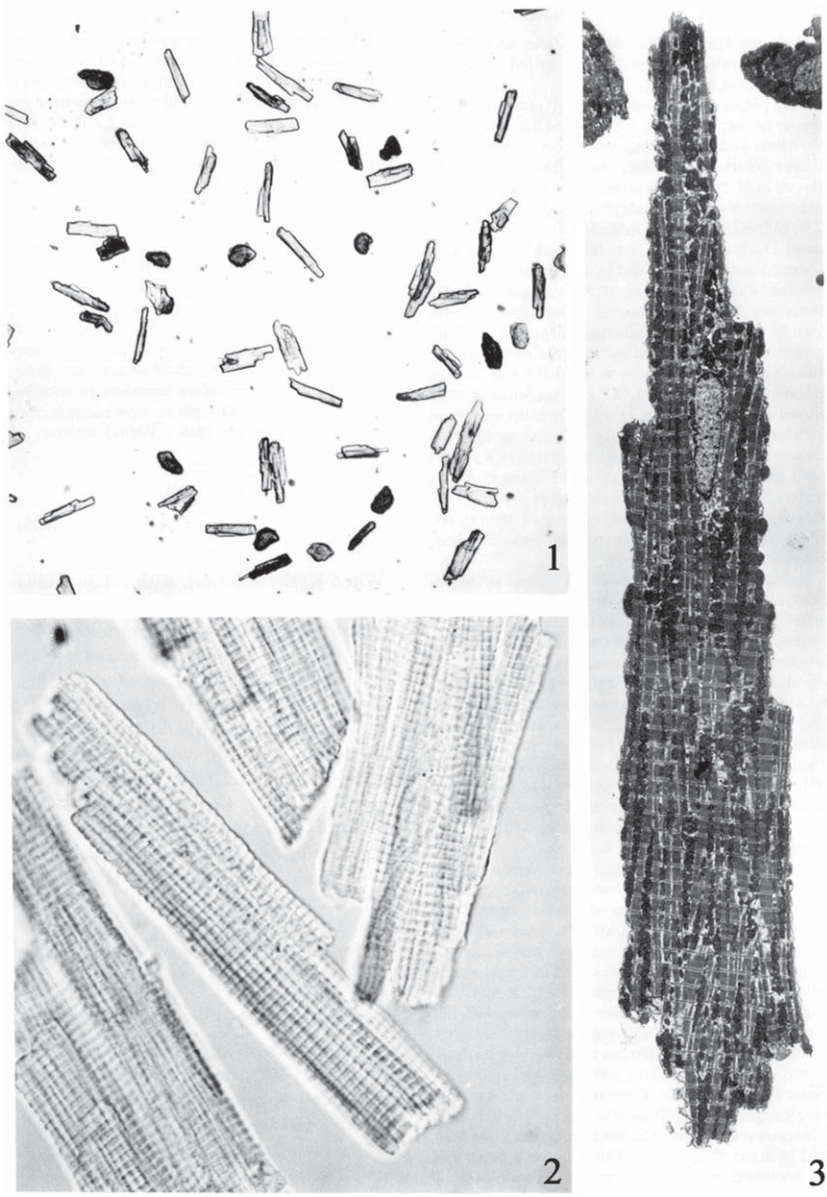

Fig. 1. **(1)** Bright-field survey view of a preparation of isolated ventricular myocytes. Damaged cells appear dark and round and are easily distinguished from the intact rod-shaped cells. (magnification ×100). **(2)** Light microscope view at higher magnification (×800) showing the structural details of rod-shaped cells. **(3)** Electron micrograph of a longitudinal thin-section through an isolated rod-shaped myocyte. Characteristic banded-structure myofilament bundles alternate between rows of mitochondria. In this example, there are 64 sarcomeres along the length of the cell. (magnification ×1500). From **ref. *25***, with permission from Elsevier.

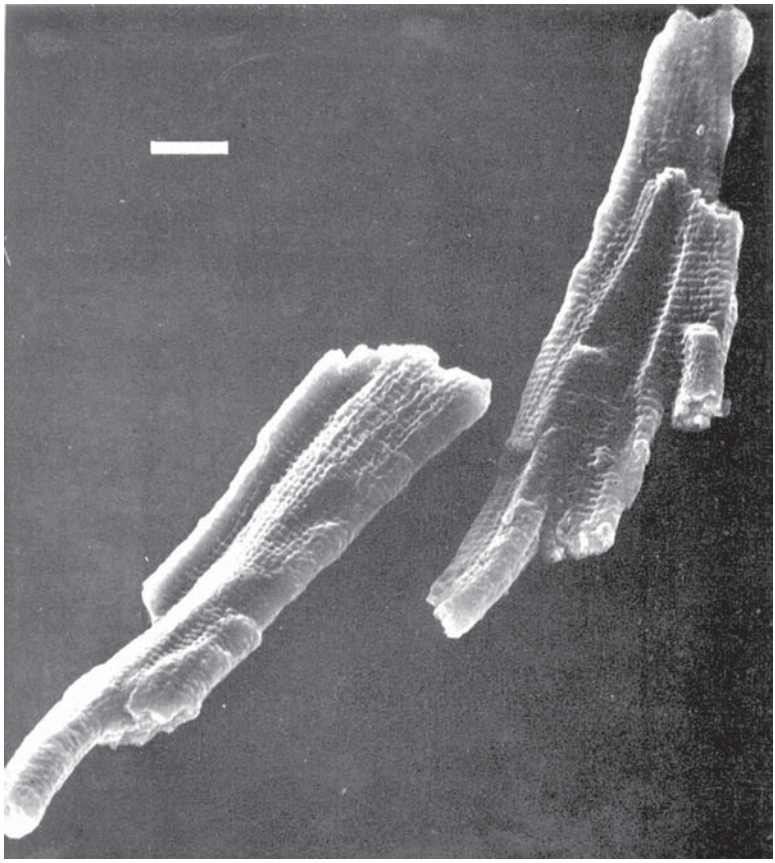

Fig. 2. The typical transverse ridges and longitudinal grooves of heart muscle cells, obtained with scanning electron microscopy. Scale bar, 10 μm (magnification ×1158). From **ref. *26***, with permission from Elsevier.

of tests (dye exclusion, morphology from low-power light microscopy and electron microscopy) that the rounded cells are myocytes damaged by the dissociation protocols. Standard purification procedures can reduce the round cell population to <10 % of the total. Of major interest are the rod-shaped cells, which display many of the gross morphological characteristics expected from studies of whole cardiac tissue. Isolated myocytes are more rectangular than cylindrical with irregular profiles, and also large, being some 80–180 μm long, 8–20 μm wide, and 8–16 μm thick. This wide range of sizes reflects the complex ventricular ultrastructure, which is illustrated more clearly by scanning electron microscopy, where individual cells are seen to be most irregular in shape (**Fig. 2**) with longitudinal grooves. On occasion, very flat cells are also

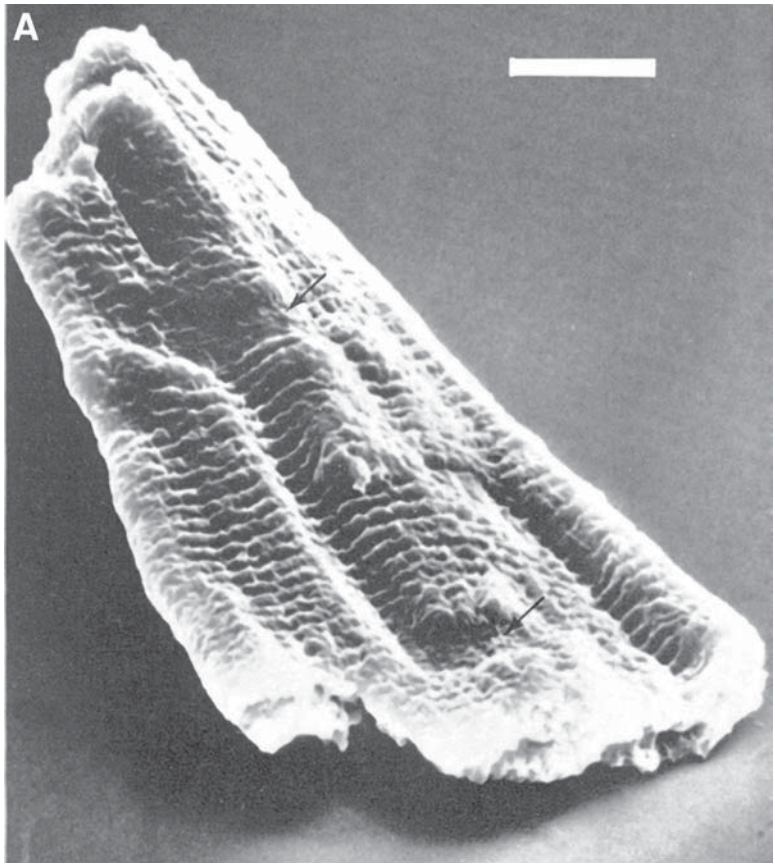

Fig. 3. **(A)** Scanning electron micrograph of cell having flatter profile than those shown in **Fig. 2**. Scale bar, 10 μm (magnification ×1158). From **ref. *26***, with permission from Elsevier.

observed (**Fig. 3A**). If it were possible to fit the cells back together again, then it becomes clear how the spiraling and horizontal bands of whole muscle (see above) arise from the complex interdigitation of myocytes with grossly varying shapes. Also apparent in **Fig. 2** are the regular transverse ridges on the surface of each cell. These reflect the action of the underlying contractile proteins, which run longitudinally within each myocyte and partially overlap, giving rise to the striated appearance of cardiac muscle, when longitudinal sections are viewed with the electron microscope (**Fig. 1**, Plate 3). As will be seen below, these general morphological features of cardiac ventricular myocytes are apparent at magnifications comfortably achievable by AFM.

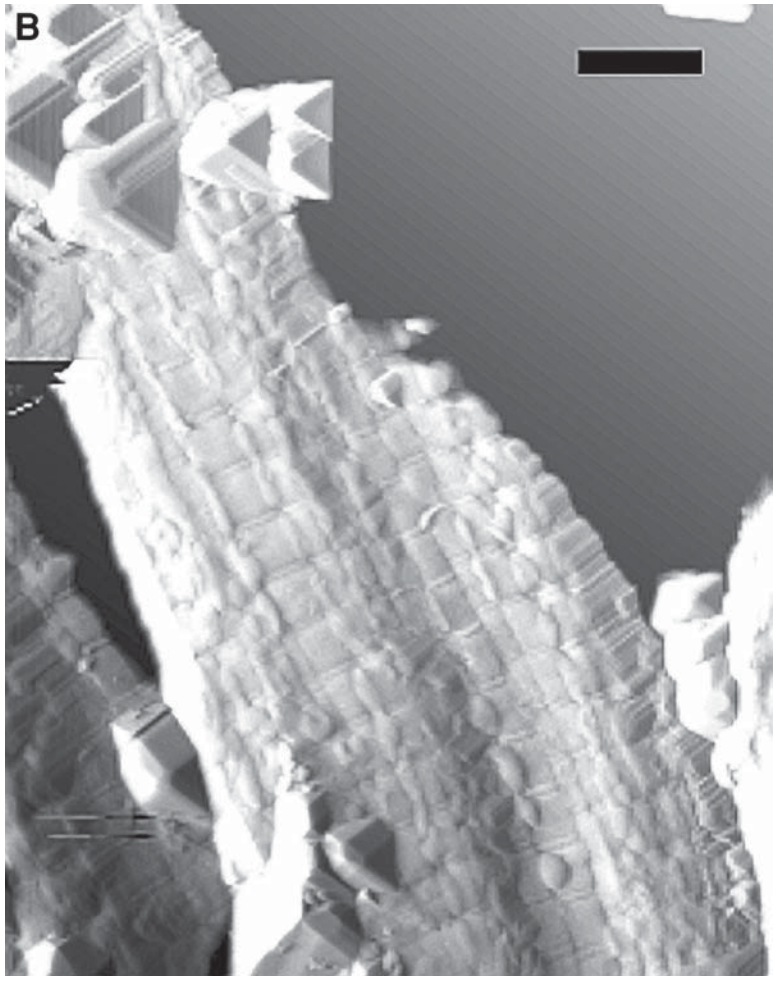

Fig. 3. **(B)** Large-scale deflection AFM micrograph of a single isolated cardiac myocyte immobilized on mica substrate. Note the intercalated disc region evident on the right-hand-side of the cell. Scale bar, 5 μm. From **ref. *9***, with permission from Elsevier.

The scalloped appearance of the surface membrane is seen in more detail in **Fig. 4A**. Evident at these levels of magnification are the regular apertures in the surface sarcolemma, the mouths of tubules dipping transversely into the cell. These T-tubules conduct the wave of electrical depolarization traveling across the myocyte surface down into the cell, so that contraction is triggered synchronously throughout the cell interior during each heartbeat. These scan-

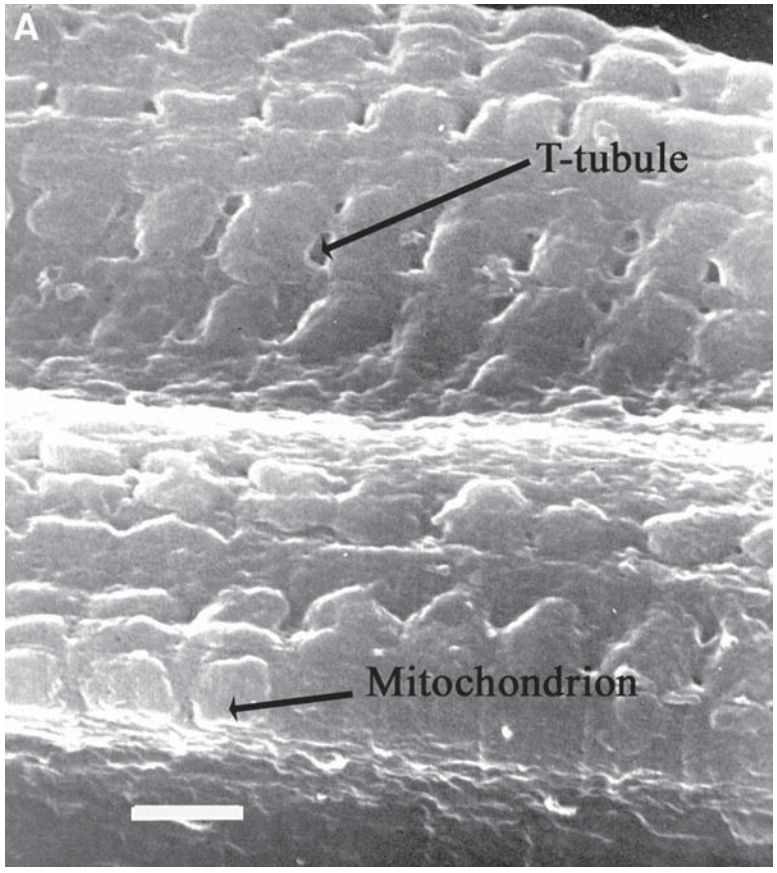

Fig. 4. **(A)** Scanning micrograph showing array of T-tubule openings, which have both ovoid and circular cross-sectional geometry. Scale bar, 2 μm (magnification ×8000). From **ref. *26***, with permission from Elsevier.

ning electron micrographs, taken on air-dried specimens of fixed myocytes, are directly relevant to observations made by AFM (see paragraphs following and **Note 2**).

Under these conditions, the surface membrane is forced down on the underlying structures, and in **Fig. 4A** there are seen rectangular "packets" at the periphery of the cell, lying along what appears to be a cylindrical structure within the cell. These packets are mitochondria, the oxidative motors in the heart, providing the aerobic production of ATP for the contractile proteins, which is essential for a normal mechanical output from each ventricle in the whole organ. It follows that if scanning force microscopy is applied to

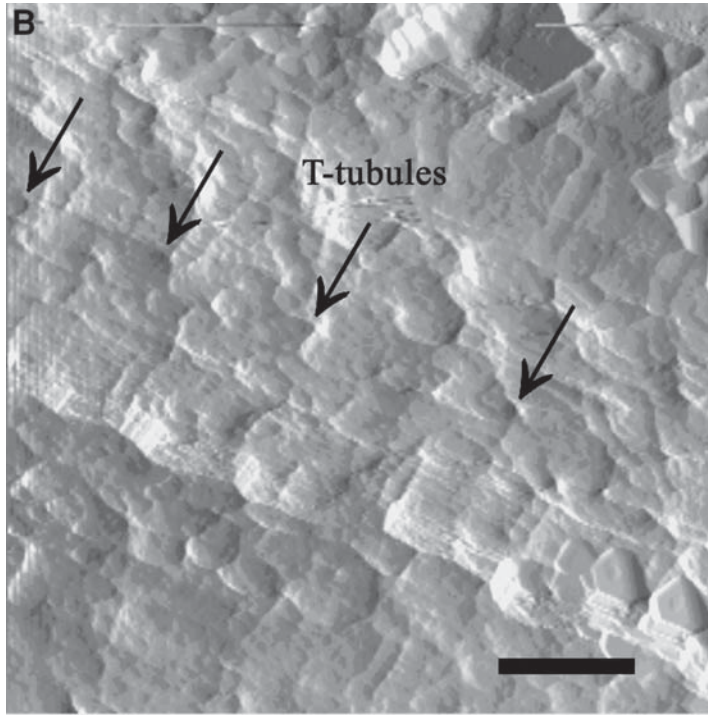

Fig. 4. **(B)** Deflection AFM micrograph of a myocyte surface in which T-tubule openings are indicated by arrows. Compressed between the contractile machinery are mitochondria. Scale bar, 2 µm. From **ref. *9***, with permission from Elsevier.

myocytes prepared using the same protocols, similar subsurface structures should be apparent (*see* **Note 3**).

Figure 5 demonstrates that all the normal features of sarcolemmal structure, including the glycocalyx, are preserved in these isolated cells. The structure of intracellular membranes and organelles also shows excellent preservation, indistinguishable from that reported in cells of the intact heart. A network of tubules in the M region, the M rete (MR), is connected by longitudinal elements (L) to a z tubule (ZT_L) seen here in longitudinal section. Examples of transversely sectioned z tubules, seen elsewhere, are indicated by ZT_T. Junctional sarcoplasmic reticulum (JSR) is continuous with the free SR (arrow) and consists of flattened cisternae closely apposed to the sarcolemma. Peripheral junctional SR (JSR_p) occurs in association with the surface sarcolemma, and interior junctional SR (JSR_I) occurs against transverse-tubule membrane. The latter may take the form of dyads (D), which consist of a transverse tubule plus one JSR cisterna, or triads (T), which consist of a transverse tubule sandwiched

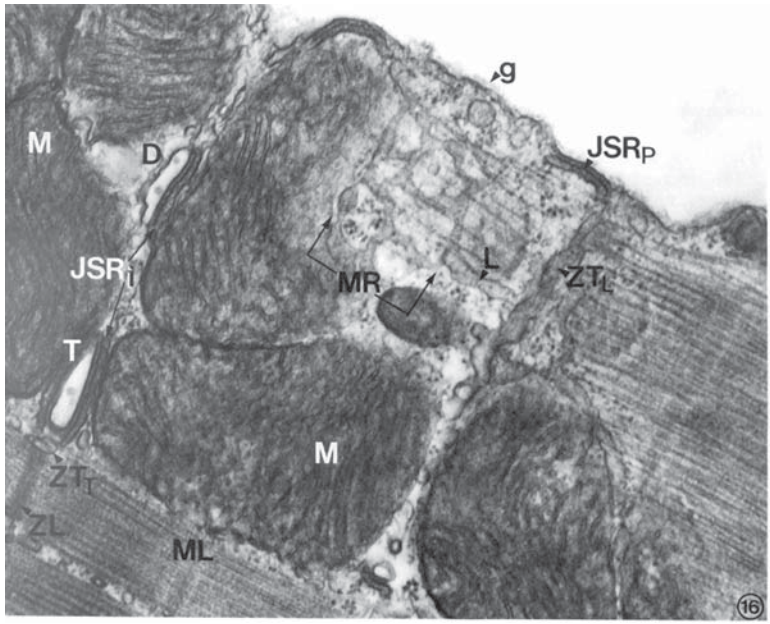

Fig. 5. Electron micrograph detailing the structural complexity of the interior of mammalian ventricular heart cells. See text for further description and abbreviations. (magnification ×50 000). D, dyad; M, mitochondria; JSR, junctional sarcoplasmic reticulum; JSR_p, peripheral JSR; L, longitudinal elements; ZT_T, transversely sectioned Z tubules; ZL, Z line; ZT_L, longitudinally sectioned Z tubule; ML, M line; g, glycalyx. From **ref. *26***, with permission from Elsevier.

between two JSR cisternae. The JSR lumen is characteristically bisected by an electron-dense line, and regularly spaced electron-dense feet project from the membrane facing the sarcolemma. Mitochondria (M) show well-preserved membranes and cristae.

Finally, if the plasma membrane is freeze-fractured, intramembrane particles can be observed (**Fig. 6**) reflecting aggregations of membrane proteins involved in cellular function; the density of these particles in isolated myocytes is very similar to that observed in whole hearts (**Fig. 7**). Note that the scale bar for these measurements (100 nm) is approaching the range more usually associated with scanning force microscopy. Clearly, freeze-fractured membranes would make most interesting specimens for AFM imaging. From the evidence presented here, and from many other studies, of those myocytes surviving the dissociation procedures, the structure of intracellular membranes and organelles shows excellent preservation, indistinguishable from that reported in cells of the intact heart.

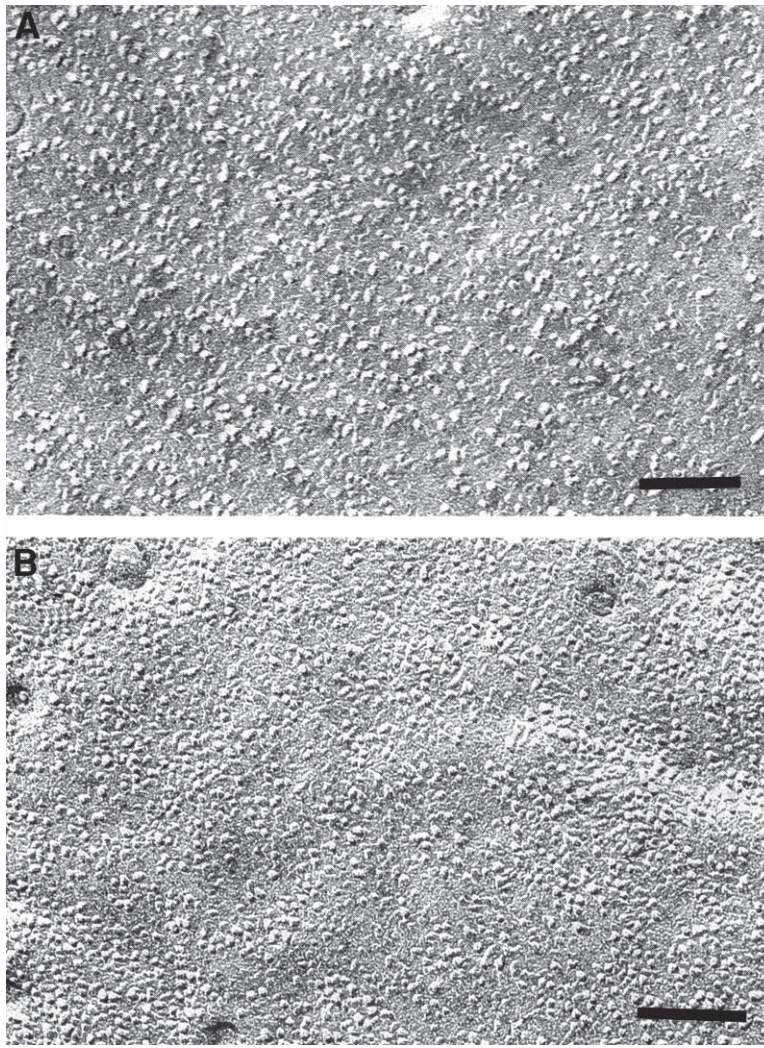

Fig. 6. **(A)** P-face view of isolated myocyte sarcolemma. **(B)** P-face view of myocyte sarcolemma from intact left-ventricular myocardium. Scale bars 0.1 µm. Taken From **ref. *27***, with permission from Elsevier.

3.2. AFM (see Notes 4–6)

Aliquots of myocytes (approx 100 µL of cell suspension) were added to a freshly cleaved mica (Agar Scientific, Cambridge, UK) surface. The sample was then gently blown dry with high purity argon or allowed to dry overnight

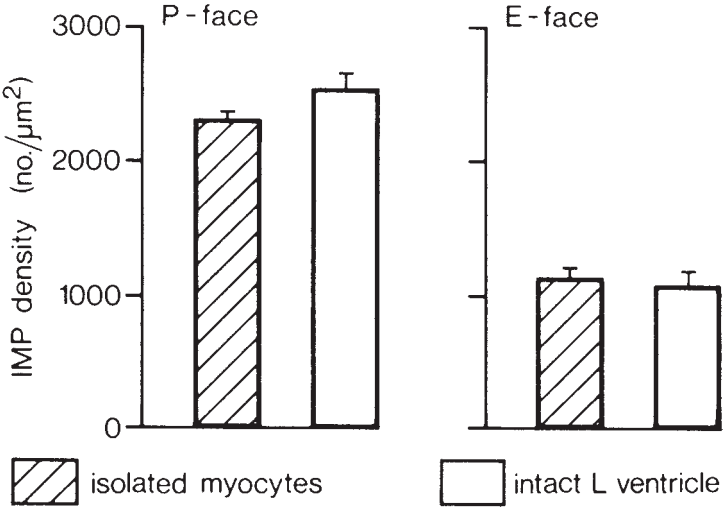

Fig. 7. Numerical density of membrane particles (expressed as numbers per square micrometer) for isolated myocytes and intact myocardium. From **ref. *27***, with permission from Elsevier.

at 5°C. Experiments were performed with a Digital Instruments MultiMode microscope in conjunction with a Nanoscope IIIa control system. A "J" scanner (with a lateral range of approximately 125 μm) was used. Etched silicon probes, attached to triangular cantilevers 100–200 μm in length, were used (Digital Instruments, UK Ltd, model TESP) operated at resonances in the 300–400 KHz range (nominal force constant 20–100 N/m). Drive amplitude was adjusted so as to give the sharpest resolution at the minimum amplitude (typically 1–2 V rms). Integral and proportional gains were balanced so as to allow simultaneous acquisition of sharp, noise-free, height and amplitude data sets. With the aid of a ×30 magnification eyepiece, the scanning cantilever was positioned directly above a surface-immobilized cell (*see* **Note 4**). Because the vertical dimensions of the cells exceed the full vertical range of the scanner (ca. 4 μm), scanning laterally into a cell commonly led to destruction of the probe. Vibrational/acoustic shielding was achieved by mounting the microscope in a PicoIsolation chamber (Molecular Imaging Co) during scanning. Height, amplitude and phase data were simultaneously collected, the latter with a Digital Instruments Phase Extender Module. Data sets were subject to a first order flattening and low band pass filtering only when stated. Thermal noise levels were estimated to be approx 0.4 Å.

As shown in **Fig. 3**, whole-cell images obtained by AFM methods compare very favorably with scanning electron micrographs. Even at this relatively low

magnification, both the cellular cross-striations and the step-like morphology of the intercalated disc regions are clearly evident. Fine details of the subsurface structure were, in general, more easily observed in deflection mode than height mode, though imaging was somewhat sensitive to the scanning set point and drive amplitude (equivalent to energy dissipation by the probe rather than the imaging force directly; *see* **Note 5**). Scanning at high amplitude produced no noticeable structural damage (though increased deformation of the plasma membrane is likely as the drive amplitude is increased), that is, when the same area was subsequently reimaged at lower drive no significant image deterioration was observed. The fact that cell dimensions exceeded the full vertical range of the scanners prevented a quantification of the effect of increased dissipation on cell height though changes in surface roughness were minimal across the range of values used. At increased magnification, the general morphology of working ventricular myocytes can be seen in more detail (**Fig. 8**). This AFM image strikingly reveals all the major characteristics of cellular morphology that have been discussed previously in reference to electron microscopy (*see* **Note 6**). The parallel arrays of longitudinal contractile machinery, separated by embedded organelles and transversed by regular tubular structures to demarcate sarcomeres, all reflect the integrated structure to be expected of this syncytial tissue.

The scalloped nature of the external sarcolemma, with the grooved surface structure reflecting the underlying contractile apparatus alternating between rows of mitochondria, is shown in **Fig. 4B**, which is presented with a corresponding scanning electron micrograph to emphasize the remarkable similarity in the two images. Z grooves, which run at right angles to the long axis of the myofilaments, mark the sarcomeres from one Z line to the next and can be quite deep and narrow, especially in contracted tissue. It is clear that there is a consistent relationship between these grooves and the Z lines, suggesting strongly that the Z line material must be attached firmly to the interior face of the plasmalemma. Using such images, resting sarcomere length is measured as 1.6–2 μm and T-tubules of diameter 200–260 nm are present in rows at approximately every 1.8–1.9 μm. The measured lateral spacing between T-tubule openings (**Fig. 4B**) is 2–2.3 μm. These dimensions are comparable to those reported for fixed ventricular cells.

4. Notes

1. It is clear that to exploit the many advantages that AFM imaging has to offer for the study of heart cells, the obvious prerequisite is a preparation of stable, isolated myocytes. Though more than 30 yr have elapsed since dissociation techniques were first reported, this initial step remains one of the most difficult. Much has been written about isolation protocols (*see* references in ***24***) and here we can

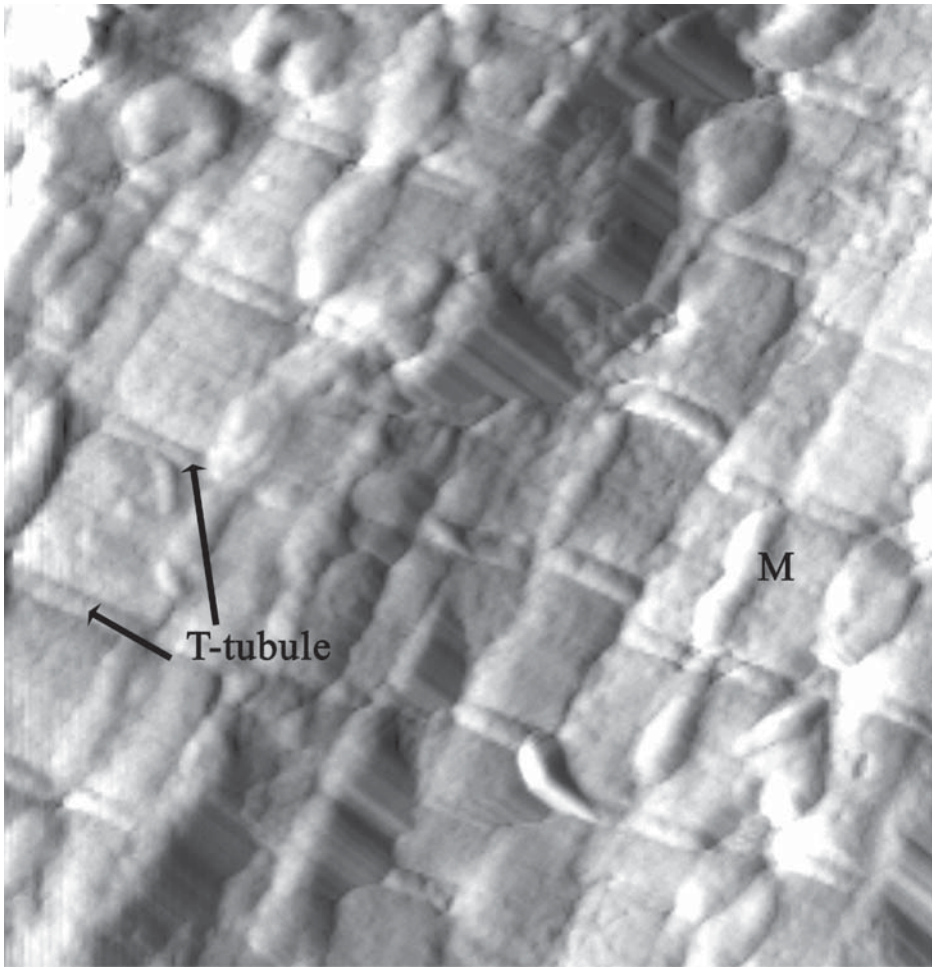

Fig. 8. High-resolution deflection AFM micrograph of a myocyte cell surface. Longitudinal columns of underlying contractile proteins, separated by valleys having regular transverse grooves. The globular features evident (M and elsewhere) are subsurface mitochondria. Also evident are the invaginations of the surface membrane by transverse tubules. Scale bar, 2 μm. From **ref. *9***, with permission from Elsevier.

give only a few of the main stumbling blocks that might prevent successful dissociation of heart tissue. The first very important procedure is retrograde coronary perfusion of the whole heart. A simple alternative would be to chop the organ and incubate the tissue chunks in the appropriate solutions, but this produces very low yields of poor quality myocytes. Cardiac tissue is predominantly aerobic, so any delay in excising and mounting the organ for in vitro perfusion can cause

irreversible damage to the constituent cells. Experience has shown that the highest-quality reagents should be used in the perfusion fluids (but not generally of spectroscopic grade) made up with high quality distilled water. Ideally, the whole dissociation protocol should be conducted in a sterile environment and the cells stored under tissue culture conditions, but as long as standard levels of cleanliness are observed, this should not be a limiting condition. Like most physiological investigations, living tissue is very susceptible to minor changes in buffer quality; therefore, new reagents should be screened before routine use. We, for example, purchase enzymes and serum albumin in bulk to minimize any major variations in myocyte quality.

2. The cells of choice should be immobilized on a flat, stable, and (ideally) optically transparent substrate surface. This may require pretreatment of cell and/or substrate surface.
3. The scanning force microscope is set up with a low spring, sharp lever and allowed to stabilize. High-powered inverted optics are used to locate the cells and carefully position the scanning probe above the one of choice. This is of particular importance with very large cells, such as cardiac myocytes, as they are typically about 8 μm thick. Tapping Probes, in particular, are expensive and easily damaged during alignment or if scanning is initiated when the tip lies to the side of a cell.
4. Surface-dried isolated myocytes are easily visible in the bright field. The cells become opaque and considerably more difficult to see in bright field on immersion in fluid. Higher optical magnification (>500×) under such conditions is of considerable benefit.
5. It is important that the cells be mechanically stable under the lateral forces imparted by the scanning probe. The worst-case scenario is when the cell is dragged across the supporting surface as scanning starts. Several imaging modes should, ideally, be available, for example, contact, noncontact, "tapping," magnetic AC ("MAC"). Each has its advantaged and disadvantages and selection should be based on maximizing resolution at minimal cellular perturbation. Occasionally, and especially in fluid, imaging will suddenly deteriorate as matter adsorbs to the scanning tip. Though commonly terminal (in terms of the tips usefulness), it may be possible to clean the probe using oxygen plasma.
6. Although surprisingly underused by physiologists and cell biologists, it is clear that AFM imaging techniques can be adapted for a large variety of cellular studies and, in terms of three-dimensional topographic resolution, compete well with classic scanning electron microscopy. By integrating AFM technology with commercially available (or adaptable) optical microscopes (such as the Nikon TE2000 inverted) one can generate a powerful imaging and characterization system. Such multiport systems can incorporate, rather straightforwardly, epi-fluorescence and confocal microscopy (with electronic motorized transfer between the two) and do not require complex set-up and alignment procedures. By integrating characterization systems in this way, it should be possible to address important questions of structure–function relationships in living cellular systems or preparations.

Acknowledgments

The authors thank The Royal Society (JJD), Abbott Diagnostics, and the EPSRC (HAOH). JJD also acknowledges The Queen's College, Oxford for an Extraordinary Junior Research Fellowship. TP is supported by the British Heart Foundation.

References

1. Kasas, S., Gotzos, V., and Celio, M. R. (1993) Observation of living cells using the atomic force microscope. *Biophys. J.* **64,** 539–544.
2. Lehenkari, P. P., Charras, G. T., Nykanen, A., and Horton, M. A. (2000) Adapting atomic force microscopy for cell biology. *Ultramicroscopy* **82,** 289–195.
3. Gunning, P. A., Kirby, A. R., Parker, M. L., Gunning, A. P., and Morris, V. J. (1996) Comparative imaging of *Pseudomonas putida* bacterial biofilms by scanning electron microscopy and both dc contact and ac non-contact atomic force microscopy. *J. Appl. Bacteriol.* **81,** 276–282.
4. Zhang, P., Bai, C., Huang, Y., Zhao, H., Fang, Y., Wang, N., and Li, Q (1995) Atomic force microscopy study of fine structures of the entire surface of red blood cells. *Scanning Microscopy* **9,** 981–988.
5. Siedlecki, C. A. and Marchant, R. E. (1998) Atomic force microscopy for characterization of the biomaterial interface. *Biomaterials* **19,** 441–454.
6. Barbee, K. A. (1995) Changes in surface topography in endothelial cells imaged by atomic force microscopy. *Biochem. Cell. Biol.* **73,** 501–505.
7. Braet, F., Seynaeve, C., de Zanger, R., and Wisse, E. (1998) Imaging surface and submembraneous structures with the atomic force microscopy: A study on living cancer cells, fibroblasts and macrophages. *J. Microscopy* **190,** 328–338.
8. Canet, D., Rohr, R., Chamel, A., and Guillian, F. (1996) Atomic force microscopy study of isolated ivy leaf cuticles observed directly and after embedding in Epon. *New Phytol.* **134,** 571–577.
9. Davis, J. J., Hill, H. A. O., and Powell, T. (2001) High resolution scanning force microscopy of cardiac myocytes. *Cell Biol. Int.* **25,** 1271–1277.
10. Hand, G. M., Muller, D. J., Nicholson, B. J., Engel, A., and Sosinsky, G. E. (2002) Isolation and characterization of gap junctions from tissue culture cells. *J. Mol. Biol.* **315,** 587–600.
11. Schar-Zammaretti, P., Ziegler, U., Forster, I., Groscurth, P., and Spichiger-Keller, U. E. (2002) Potassium-selective atomic force microscopy on ion-releasing substrates and living cells. *Anal. Chem* **74,** 4269–4274.
12. Braunstein, D. and Spudich, A. (1994) Structure and activation dynamics of RBL-2H3 cells observed with scanning force microscopy. *Biophys. J.* **66,** 1717–1725.
13. Schoenberger, C. A. and Hoh, J. H., (1994) Slow cellular dynamics in MDCK and R5 cells monitored by time-lapse atomic force microscopy. *Biophys. J.* **67,** 929–936.
14. Schauss, S. S. and Henderson, E. R. (1997) Cell viability and probe-cell membrane interactions of XR1 glial cells imaged by atomic force microscopy. *Biophys. J.* **73,** 1205–1214.

15. Haydon, P. G., Lartius, R., Parpura, V., and Marchese-Ragona, S. P. (1996) Membrane deformation of living glial cells using atomic force microscopy. *J. Microscopy* **182,** 114–120.
16. Klebe, R. J., Bentley, K. L., and Schoen, R. C. (1981) Adhesive substrates for fibronectin. *J. Cell. Physiol.* **109,** 481–488.
17. Butt, H. J., Wolff, E. K., Gould, S. A. C., Northern, B. D., Peterson, C. M., and Hansma, P. K. (1990) Imaging cells with the atomic force microscope. *J. Struct. Biol.* **105,** 54–61.
18. Kasas, S. and Ikai, A. (1996) A method for anchoring round shaped cells for atomic force microscope imaging. *Biophys. J.* **68,** 1678–1680.
19. Gab, M. and Ikai, A. (1996) Method for immobilizing microbial cells on gel surface for dynamic AFM studies. *Biophys. J.* **69,** 2226–2233.
20. Yamashina, S. and Shigeno, M. (1995) Application of atomic force microscopy to ultrastructural and histochemical studies of fixed and embedded cells. *J. Electron Microsc.* **44,** 462–466.
21. Zhang, Y., Sheng, S. J., and Shao, Z. (1996) Imaging biological structures with the cryo atomic force microscope. *Biophys. J.* **71,** 2168–2176.
22. Hoh, J. H. and Schonenberger, C. A. (1994) Surface morphology and mechanical properties of MDCK monolayers by atomic force microscopy. *J. Cell. Sci.* **107,** 1105–1114.
23. Domke, J., Parak, W. J., George, M., Gaub, H. E., and Radmacher, M. (1999) Mapping the mechanical pulse of single cardiomyocytes with the atomic force microscope. *Eur. Biophys. J. Biophys Lett.* **28,** 179–186.
24. Powell, T., Noma, A., and Severs, N.J. (1998) Isolation and culture of adult cardiac myocytes, in *Cell Biology: A Laboratory Handbook*, 2nd ed, vol. 1 (Celis, J. E., ed). Academic Press, San Diego, CA, 1pp. 25–132:
25. Severs, N. J., Slade, A. M., Powell, T., Twist, V. W., and Warren, R. L. (1982) Correlation of ultrastructure and function in calcium-tolerant myocytes isolated from the adult rat heart. *J. Ultrastruct. Res.* **81,** 222–239.
26. Powell, T., Steen, E.M., Twist, V.W., and Woolf, N. (1978) Surface characteristics of cells isolated from adult rat myocardium. *J. Mol. Cell. Cardiol.* **10,** 287–292.
27. Slade, A. M., Severs, N. J., Powell, T., Twist, V. W., and Jones, G. E. (1985) Morphometric analysis of calcium-tolerant myocytes isolated from the adult rat heart, in *Advances in Myocardiology*, vol. 6 (Dhalla, N. S. and Hearse D. J., eds.), Plenum Publishing Corporation, New York, pp. 3–12.